Pergamon

Journal of Structural Geology, Vol. 17, No. 12, pp. 1673 to 1688, 1995
Elsevier Science Ltd
Printed in Great Britain

0191-8141(95)00061-5

A structural record of the emplacement of the Pozanti–Karsanti ophiolite onto the Menderes–Taurus block in the late Cretaceous, eastern Taurides, Turkey

ALI POLAT* and JOHN F. CASEY

University of Houston, Department of Geosciences, Houston, TX 77204, U.S.A.

(*Received* 17 *November* 1994; *accepted in revised form* 15 *May* 1995)

Abstract—The Aladag region of eastern Taurides, Turkey, is characterized by an imbricated thrust structure developed during late stage emplacement of the Pozanti–Karsanti ophiolite onto the Menderes–Taurus block in the late Cretaceous. The mid to late Cretaceous dynamothermal metamorphic sole and the underlying unmetamorphosed mélange, here named the Aladag accretionary complex, were accreted to the base of the Pozanti–Karsanti ophiolite during intra-oceanic subduction, transport and final obduction of the ophiolite onto the Menderes–Taurus block.

In the dynamothermal metamorphic sole, intensity of deformation and degree of metamorphism increase from the base to the top, and at least three episodes of foliation, lineation and fold development are recognized. The asymmetry of quartz *c*-axis fabrics, tightness and asymmetry of folds of the same generation, and curvature of fold hinge lines increase from base to top, indicating that non-coaxial progressive deformation prevailed during the development of the metamorphic sole. The mélange is divided into three major thrust fault-bounded tectonic slivers, each of which is characterized by distinctive types of matrix and block lithologies, structures and deformation style. Kinematic analyses of the dynamothermal metamorphic sole and the mélange reveal that the tectonic transport direction of the Pozanti–Karsanti ophiolite during its emplacement was from north-northwest to south-southeast, suggesting that the Pozanti–Karsanti ophiolite was derived from a Neo-Tethyan ocean to the north of the Menderes–Taurus block.

INTRODUCTION

Ophiolite complexes contain a distinct assemblage of mafic to ultramafic rocks and are believed to represent fragments of oceanic lithosphere (Coleman 1977, Nicolas 1989). Plate convergence episodes, which generally culminate in continental collisions, may be recorded in ophiolites and related rocks. The emplacement of ophiolites has been described by many authors in terms of plate tectonics (Coleman 1971, Dewey & Bird 1971, Dewey 1976, Moores 1982, Casey & Dewey 1984, Searle & Stevens 1984, Sengör 1990a). However, why, how and where the detachment of oceanic lithosphere begins, and mechanisms by which ophiolites are emplaced onto less dense continental margins, are still poorly understood. Moores (1982) divided ophiolites into two groups: Tethyan and Cordilleran. Most Tethyan-type ophiolites contain a poly-deformed dynamothermal metamorphic sole, with an inverted metamorphic gradient ranging from amphibolite facies at the top to greenschist facies at the bottom, and are the highest thrust nappes resting on structurally lower sedimentary nappes and passive continental margin sequences (e.g. Semail, Kizildag, Baër–Bassit, and Pozanti–Karsanti ophiolites). These ophiolites are considered obducted because they originated as upper plate fore-arc massifs (Moores 1982, Hacker 1990). Cordilleran-type ophiolites, on the other hand, are smaller and often occur as trapped fragments within accretionary wedges; they are considered subducted since they involve transfer of oceanic crust from the subducting oceanic lithosphere to the overriding plate (e.g. Knight Island ophiolite—Alaska).

The emplacement events and mechanism of emplacement (e.g. kinematics) are best recorded by deformation and associated metamorphism within the ophiolites themselves and in appended dynamothermal metamorphic soles and underlying mélanges (Williams & Smyth 1973, Searle & Stevens 1984, Jamieson 1986, Robertson *et al.* 1990). Therefore, determination of the structural evolution of dynamothermal metamorphic soles and mélanges will provide critical insight into emplacement histories of ophiolites (Spray 1984, Shackleton *et al.* 1990).

In this study, the dynamothermal metamorphic sole and the underlying mélange beneath the Pozanti–Karsanti (P–K) ophiolite are defined as high and low temperature divisions, respectively, of an obduction-related Neo-Tethyan accretionary complex. The structural fabrics in the dynamothermal metamorphic sole and mélange are not only excellent kinematic indicators, but also provide significant information on the types of deformation mechanisms and change in the strain rates during their formation. The purpose of this paper is to study the kinematic history of emplacement of the P–K ophiolite onto the Menderes–Taurus (M–T) continental block by using macroscopic, mesoscopic and microscopic structures of the dynamothermal metamorphic sole and the Aladag mélange, and to re-examine the geological history of the region.

*Current address: University of Saskatchewan, Department of Geological Sciences, Saskatoon, Saskatchewan, Canada, S7N 0W0.

GEOLOGICAL SETTING

Northeastward translation of Africa towards Eurasia due to the opening of the South Atlantic in the early Cretaceous resulted in detachment of several Neo-Tethyan ophiolites (e.g. Oman, Kizildag, Baër–Bassit and P–K ophiolites) in the eastern Mediterranean region either at spreading ridges or transform plate boundaries, and obduction of these ophiolites onto passive continental margins of the Arabian and Anatolide–Tauride platforms in the Late Cretaceous (Robertson & Dixon 1984, Dercourt *et al.* 1986, Dewey 1988, Hacker 1990). The P–K ophiolite represents one of the largest fragments of oceanic lithosphere in Turkey. It is located in the Aladag region, in the eastern Taurus mountains of southern Turkey, between the left-lateral Ecemis strike-slip fault to the west, and the Bitlis suture zone and left-lateral east Anatolian strike-slip fault to the east (Fig. 1).

The rocks in the region preserve the record of the opening and closure of a Neo-Tethyan ocean, termed 'the inner-Tauride Ocean' (Sengör & Yilmaz 1981, Sengör 1990b), that existed in the Mesozoic between the M–T and Kirsehir continental blocks. Sengör (1990b) suggested that the separation of the M–T continental block from the Kirsehir block had taken place by the Early Triassic as the inner-Tauride ocean started to open, possibly as a back arc basin behind the Podataksasi zone (Fig. 2). The M–T block had formed a part of northern Gondwanaland until Middle Triassic times. Its rifting from the Arabian platform is marked by extensive volcanism of mainly Carnian age (Sengör & Yilmaz 1981, Delaloye & Wager 1984, Robertson & Dixon 1984, Whitechurch *et al.* 1984). The inner-Tauride ocean was consumed by the pre-terminal collision (prior to the closure of the inner-Tauride ocean) between the forearc P–K ophiolite and the M–T block in the Late Cretaceous, and the following terminal continent–continent collision between the Kirsehir block and the M–T block along the intra-Tauride suture zone during the late Palaeocene–early Eocene (Sengör & Yilmaz 1981, Görür *et al.* 1984).

TECTONOSTRATIGRAPHY

An imbricated stack of thrust sheets resting upon the eastern Taurus autochthon is exposed in the Aladag region (Fig. 3; Blumenthal 1947, Tekeli *et al.* 1983). The upper thrust sheets are composed of allochthonous units consisting of the early to mid Cretaceous P–K ophiolitic complex with a Turonian–Santonian dynamothermal metamorphic sole, and the underlying late Campanian to Maastrichtian Aladag mélange (Fig. 3; Tekeli 1983, Tekeli *et al.* 1983). The lower thrust sheets are composed of para-autochthonous units, including platform-type carbonates of late Devonian through early Cretaceous age, which formed at sites more proximal to the M–T margin (Tekeli *et al.* 1983).

The presently exposed P–K ophiolite extends more than 100 km from the left-lateral Ecemis strike-slip fault in the southwest, to Burhaniye in the northeast, and is up to 30 km wide (Fig. 1). The ophiolite is primarily composed of dunite, harzburgite and gabbro, and this crustal section (sheeted dyke complex and pillow lava sequence) was eroded during and after its emplacement onto the M–T block (Whitechurch *et al.* 1984). Discontinuous or continuous sequences of dynamothermal metamorphic sole and ophiolitic mélange are exposed beneath the P–K ophiolite as are typically found in association with other Tethyan-type ophiolites. The dynamothermal metamorphic sole is the thrust zone at the base of the ophiolite, comprising upper amphibolite facies at the top and greenschist facies rocks at the base. The mélange is composed of a variety of igneous, metamorphic and sedimentary blocks structurally dispersed in a serpentinitic to pelitic matrix. The style of deformation in the mélange varies from ductile at the top to brittle at the base. The nature of the contact between the mélange and underlying para-autochthonous carbonates was interpreted as a depositional contact by Tekeli (1981) and Tekeli *et al.* (1983). This interpretation, however, is not supported by the field relationships and geological history of the region as discussed in the following sections.

The para-autochthonous units can be divided into six imbricated thrust sheets (Tekeli *et al.* 1983). These thrust sheets, from structurally lowest to structurally highest, are: (1) the Yahyali thrust sheet, which includes intensively deformed and metamorphosed, at low grades, Upper Palaeozoic–Mesozoic sequences; (2) the Siyah (Black) Aladag thrust sheet, which is composed of Upper Palaeozoic–Middle Triassic sequences; (3) the Minaretepeler thrust sheet, which consists of Upper Triassic–Lower Jurassic sequences; (4) the Cataloturan thrust sheet, which includes Upper Palaeozoic–Lower Mesozoic sequences; (5) the Beyaz (White) Aladag thrust sheet, which contains a thick dolomitic limestone sequence of Middle Triassic–Lower Cretaceous age; and (6) the Divrik Dagi thrust sheet, which is characterized by Upper Jurassic–Lower Cretaceous carbonates (Fig. 3). There is no obvious relationship between the age of the rocks in the thrust sheets and imbrication order, suggesting that the present thrust sequence resulted from a complicated out-of-sequence thrusting event which took place during final emplacement of the ophiolite. The overthrusting direction is recorded by south–southeast facing overturned folds and associated thrust faults within both the allochthonous and para-autochthonous sheets.

DYNAMOTHERMAL METAMORPHIC SOLE

The dynamothermal metamorphic sole is composed of amphibolite facies rocks at the top and greenschist facies rocks at the base, and has a tectonostratigraphic thickness of about 460 m in the northern Ulupinar valley (Fig. 4). The amphibolite facies is predominantly metavolcanic rocks, whereas the greenschist facies is composed of both metavolcanic and metasedimentary rocks.

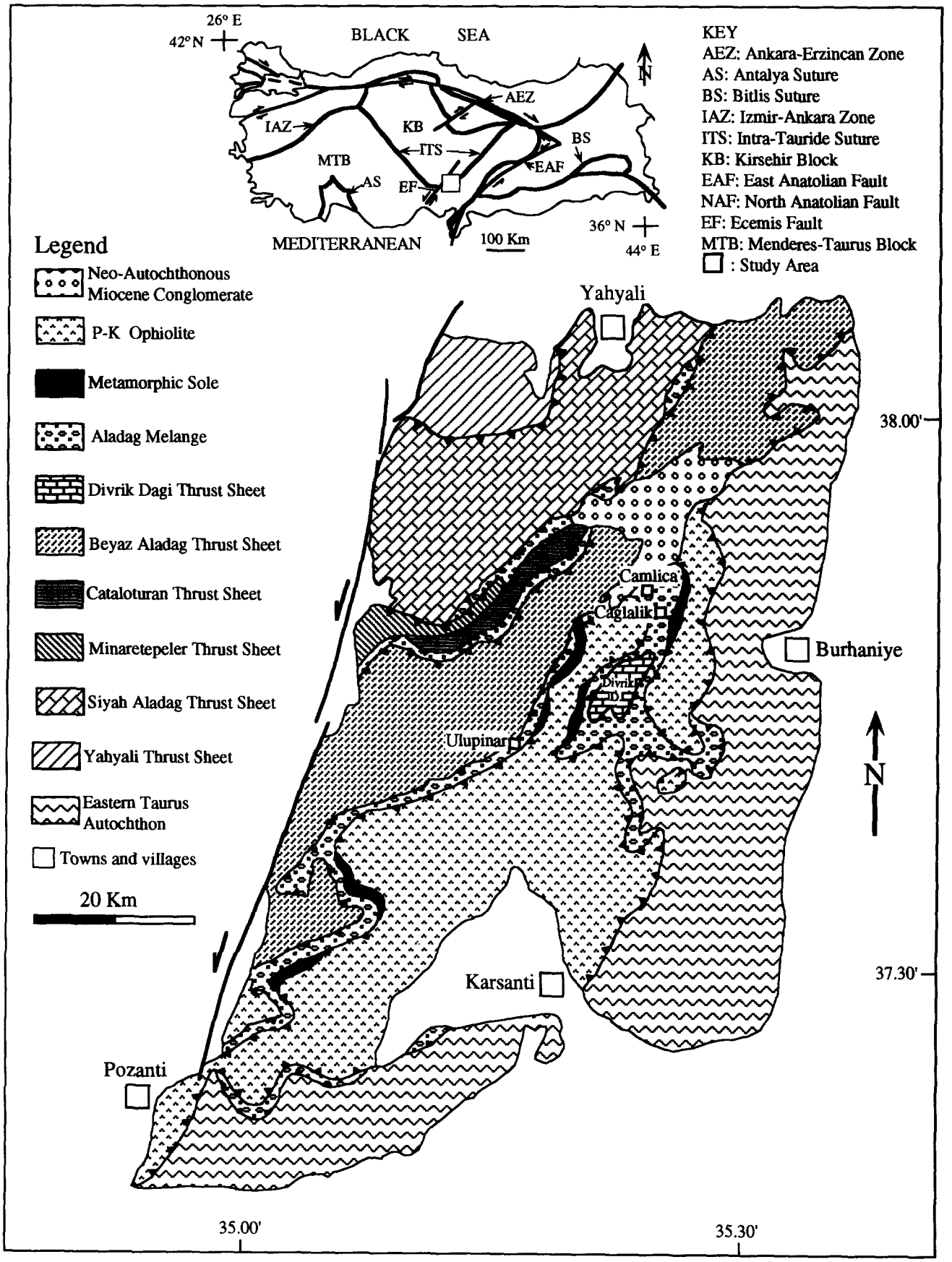

Fig. 1. Regional geological map of the study area. The Aladag region is located on the intra-Tauride suture (ITS) zone which developed during the Neo-Tethyan evolution of Turkey (modified after Tekeli *et al.* 1983).

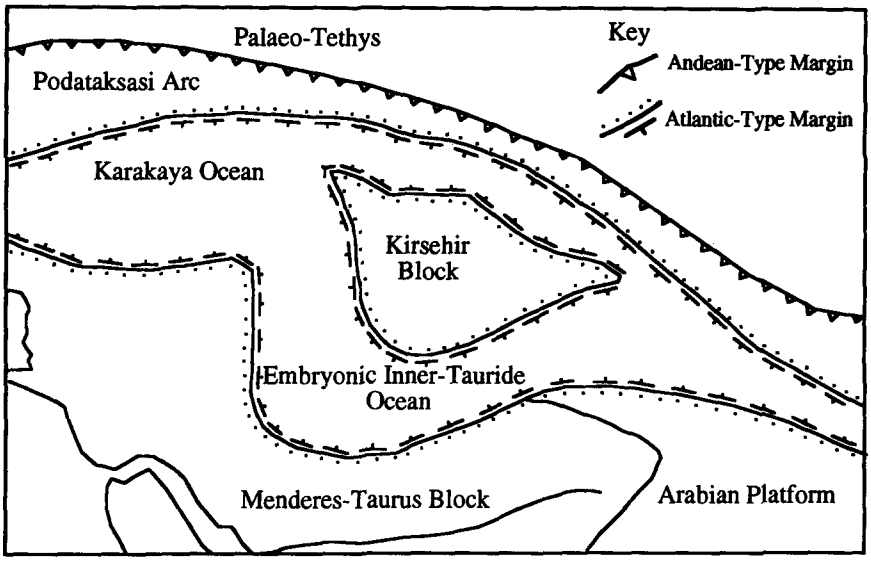

Fig. 2. Simplified Palaeogeographic map of the eastern Mediterranean region for early Triassic time, showing the opening of the 'Inner-Tauride ocean' between the Kirsehir and Menderes–Taurus continental blocks behind 'the Podataksasi zone' (modified after Sengör 1990a).

Geochemical investigation of the dynamothermal metamorphic sole suggests that the majority of volcanic rocks in the amphibolite facies were derived from an alkali ocean island basalt (OIB) protolith, whereas metavolcanic sequences within the greenschist facies were derived from 'normal' mid-ocean ridge basalt (N-MORB). Metasedimentary rocks of the greenschist facies, which are dominantly metapelites and metacherts, were derived from abyssal plain pelagic sedimentary protoliths (Polat 1992).

The dynamothermal metamorphic sole and the ophiolite are crosscut by 0.5–3 m thick dykes of mafic to intermediate composition, which postdate the metamorphism. Their mineralogy is dominated by quartz, hornblende and plagioclase. These dykes yield an age of 70–75 Ma, whereas amphibolite facies rocks of the sole yield an age of 90–94 Ma (K–Ar method; Thuizat *et al.* 1981).

The dynamothermal metamorphic sole tectonically underlies the residual mantle section of the P–K ophiolite and is tectonically underlain by the Aladag mélange. The contact between the metamorphic sole and the overlying ophiolite is defined by a 3–6 m thick serpentinitic mantle tectonite, which represents the intra-oceanic decoupling surface; it is well exposed in the vicinity of northern Ulupinar and southern Caglalik villages (Fig. 5). The schistosity in the serpentinized mantle tectonites is sub-parallel to the contact and to the schistosity in the amphibolite and greenschist facies rocks. The lithologic variation and mineral paragenesis of the dynamothermal metamorphic sole are shown in Fig. 4.

STRUCTURES OF THE DYNAMOTHERMAL METAMORPHIC SOLE

Foliation

The entire dynamothermal metamorphic sole has experienced a history of foliation development both at the mesoscopic and microscopic scales. Two types of planar structures, such as metamorphic compositional layering and cleavage, characterize the foliation in the dynamothermal metamorphic sole. Intensity and degree of development of these structures vary from facies to facies, as well as from lithology to lithology in the same facies. In general, foliation development is more pronounced in greenschist facies rocks than in amphibolite facies rocks. In the greenschist facies rocks, the intensity and number of foliation systems tend to increase from base to top, whereas in the amphibolite facies rocks this vertical gradient of fabric intensity is not clear.

A widely spaced, SE-dipping metamorphic compositional layering, with a thickness ranging from a few mm to several cm, is the only foliation that can be defined at the base of the section. Towards the top, the foliation becomes more closely spaced and new foliation systems begin to appear.

At least three distinctive cleavage systems are recognized in outcrops of the Ulupinar and Caglalik regions (Fig. 5). A moderately SE-dipping, NE-striking S_1 cleavage, which is typically associated with metamorphic compositional layering both in the greenschist and amphibolite facies rocks, is the most readily recognizable foliation throughout much of the dynamothermal metamorphic sole (Fig. 6). It tends to be well-developed within the metapelites and metavolcanic rocks, and is poorly developed within the metacherts. In the metapelites of greenschist facies, metamorphic compositional layering is characterized by domains rich in phyllosilicates such as muscovite and chlorite (P-domains) and by domains rich in quartz (Q-domains). In the uppermost greenschist division, the Q-domains have undergone boudinage, forming pinch and swell structures (Fig. 6). In the metavolcanic rocks of the greenschist facies, S_1 cleavage is more closely spaced than in the metapelites, and metamorphic compositional layering is defined by domains rich in chlorite and epidote and domains rich in feldspar and quartz.

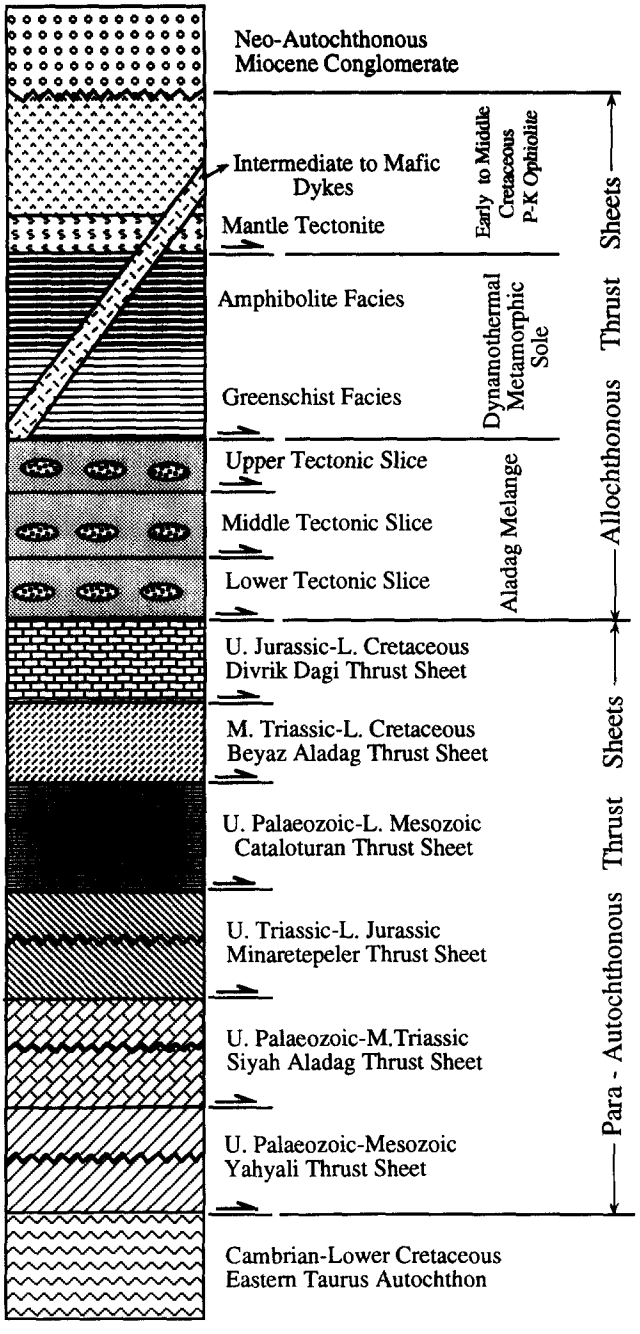

Fig. 3. Tectonostratigraphy of the Aladag region, indicating that the area is characterized by thrust structures developed during the late stage emplacement of the Pozanti–Karsanti ophiolite onto the Menderes–Taurus block in the late Cretaceous.

Metamorphic compositional layering and associated S_1 cleavage are the dominant foliations within the amphibolite facies rocks. In the amphibolites, compositional layering is characterized by hornblende and plagioclase domains, whereas in the gneisses compositional layering is defined by domains rich in quartz and feldspar and domains rich in muscovite.

Steeply NW-dipping, NE-striking S_2 crenulation cleavage, which generally tends to occur as an axial planar cleavage to F_1 folds, occurs throughout the metamorphic sole, but it is more pronounced within greenschist facies rocks.

Steeply SW–NE-dipping, NW-striking S_3 cleavage, which crenulates both the S_1 and S_2 fabrics, is mainly restricted to the greenschist facies, and appears to have resulted from microscopic- and mesoscopic-folding and fracturing (cf. Rajlich 1991). The S_3 cleavage is less closely spaced compared with S_1 and S_2 cleavages.

Lineation

The entire dynamothermal metamorphic sole has a well-developed mineral stretching lineation trending predominantly NW–SE. During the development of foliations, hornblende and plagioclase in the amphibolites, muscovites in the gneisses of the amphibolite facies rocks, and chlorite and muscovite in the greenschist facies rocks, were oriented in the foliation planes to form stretching lineations. In the greenschist facies rocks, stretching mineral lineations, L_1, L_2 and L_3, lie in the S_1, S_2 and S_3 foliation planes, and tend to be oriented perpendicular to the fold axes. It is not clear, however, whether the L_2 and L_3 stretching lineations were developed by the mechanical rotation of the L_1 stretching lineation or grew independently during post-S_1 metamorphism and deformation.

The dominant mineral stretching lineation throughout much of the amphibolite facies is L_1 and it is generally associated with S_1 foliation; it tends to parallel the fold axial planes at high angles to the fold axis. It is difficult to distinguish L_2 and L_3 lineations from L_1 lineation in the amphibolites. This is probably partly due to recrystallization of hornblende in the same orientation during the subsequent deformation and metamorphism, or partly due to absence of well-developed S_2 and S_3 foliations in these rocks.

Folding

Complex folding is the most striking manifestation of multiphase deformation in the dynamothermal metamorphic sole. At least three episodes of folding have been recognized both in the greenschist and amphibolite facies (Fig. 7). Their amplitude ranges from a microscopic scale to several metres, and their tightness ranges from open to isoclinal. In the greenschist facies rocks, non-cylindrical F_1 folds are close to isoclinal, usually asymmetric and overturned to the SE, with NW-dipping axial planes and horizontal to gently NE-plunging fold hinge lines. These folds are commonly accompanied by well-developed S_2 axial planar cleavage. Towards the top of the greenschist facies rocks, the magnitude of the interlimb angles of the F_1 folds decreases, whereas the degree of their asymmetry increases. The SE-plunging, noncylindrical recumbent F_1 folds within amphibolite facies rocks are predominantly isoclinal. Their axial planes are parallel to the S_1 metamorphic compositional layering, and fold hinge lines are curved into an arc shape, resembling sheath folds.

The NE-trending, non-cylindrical F_2 folds in the greenschist facies rocks are close to tight, and are typical of Z and S asymmetric folds occurring on the limbs of the F_1 folds (Fig. 7). In the amphibolite facies rocks, noncylindrical F_2 folds are close to isoclinal, with horizontal

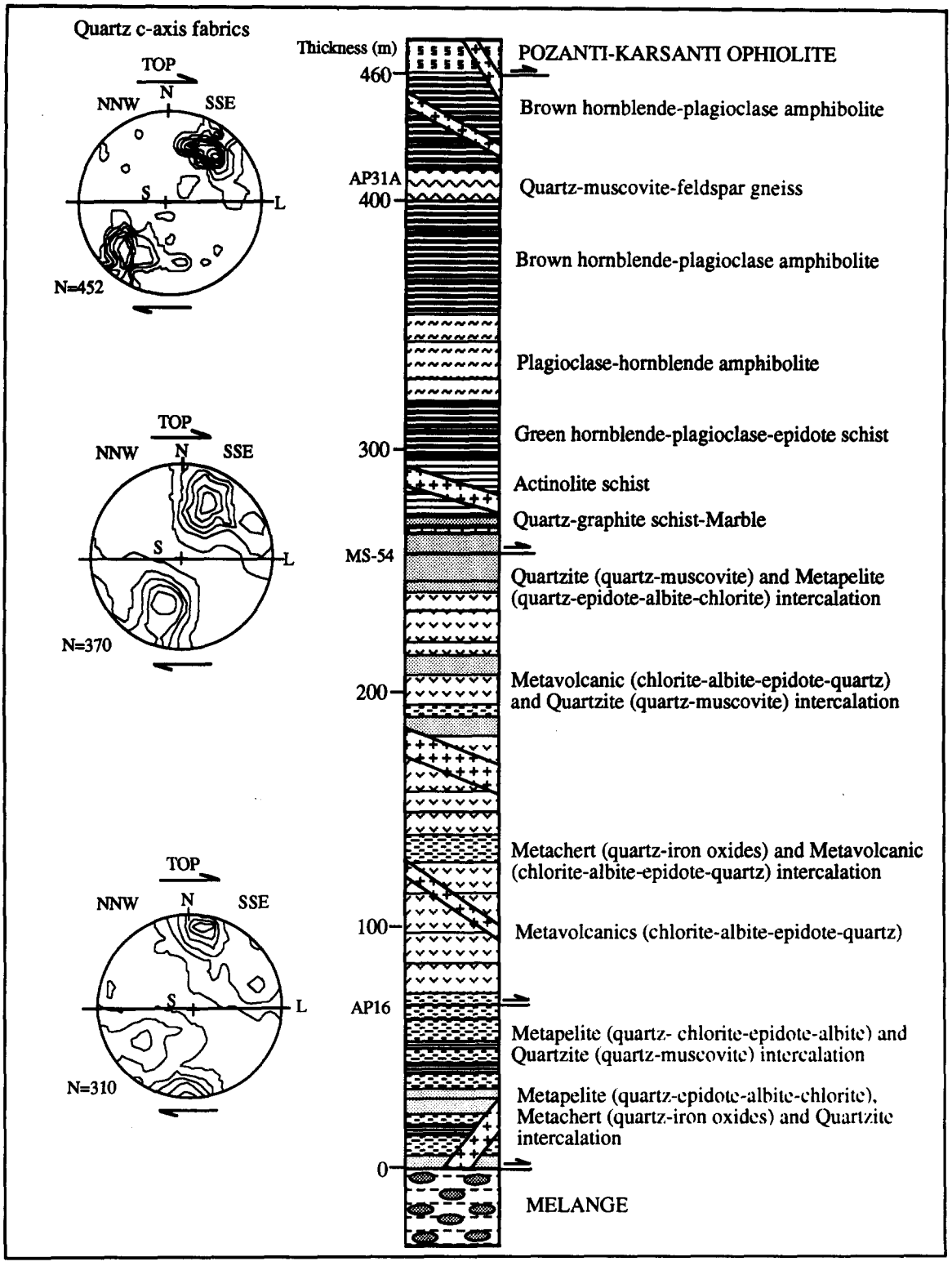

Fig. 4. Measured tectonostratigraphic section of the dynamothermal metamorphic sole in the northern Ulupinar valley. Metamorphic grade ranges from greenschist at the base to amphibolite facies at the top. Quartz *c*-axis fabrics and related sample locations are shown on the left; contour interval for the quartz *c*-axis fabrics is 1% per 1% area. The *S* and *L* represent the foliation and stretching lineations, respectively.

to gently SE-dipping axial planes, and have larger amplitudes compared with the F_1 folds. The F_3 folds of the greenschist facies rocks are generally open with horizontal to gently SE-dipping axial planes and horizontal to gently NE-plunging hinge lines. The F_3 folds in the amphibolite facies rocks are open to close, with steeply NW–SE-dipping axial planes and horizontal to gently plunging, NE–SW-trending hinge lines (Fig. 7).

Because the intensity of folding decreased during the development of the dynamothermal metamorphic sole, the main character of the early folds is not obscured significantly by superimposed folds; thus, it is possible to

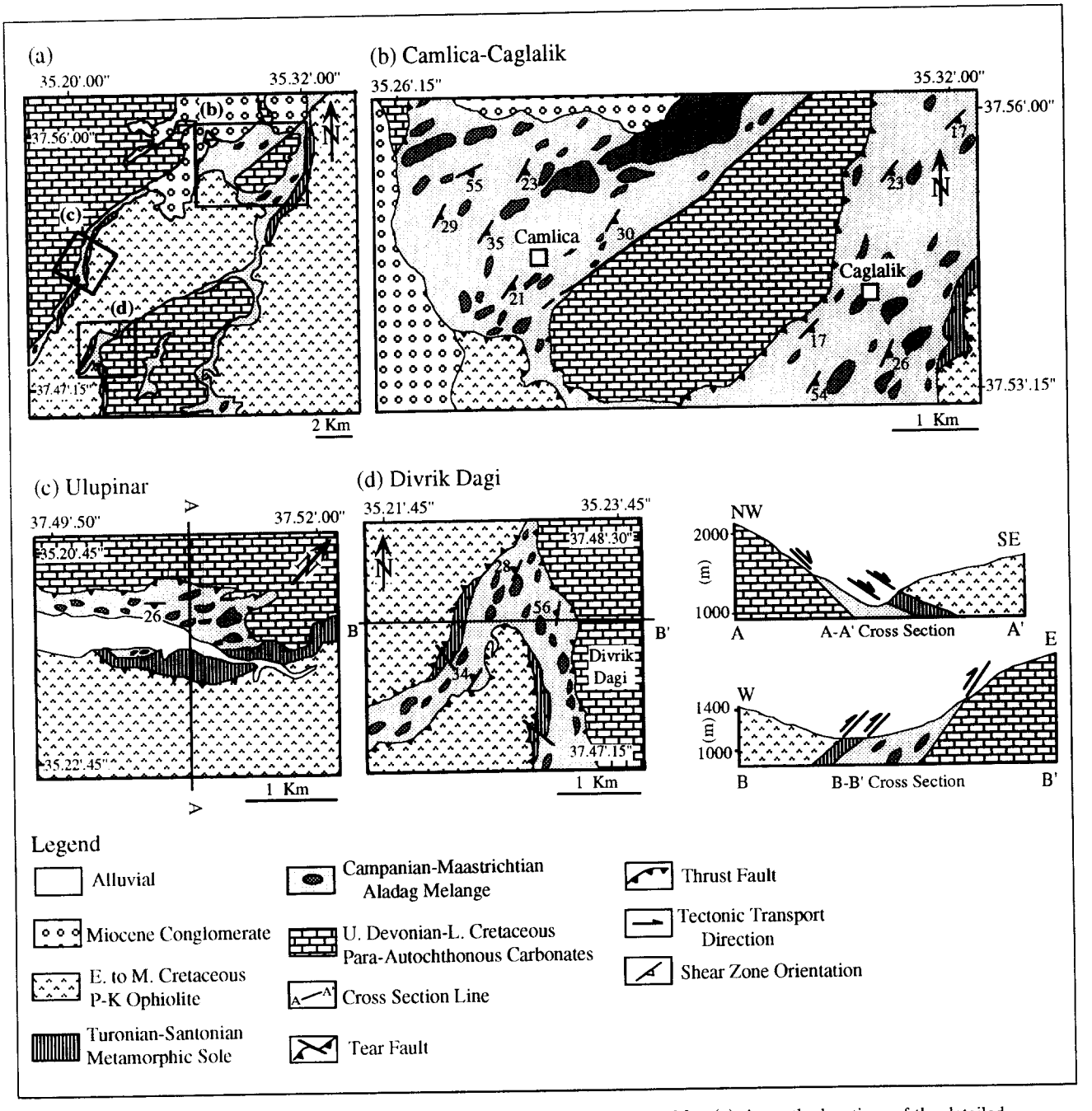

Fig. 5. Detailed geological maps and interpreted cross-sections of the area. Map (a) shows the locations of the detailed investigation areas of (b) the Camlica–Caglalik, (c) Northern Ulupinar and (d) Divrik Dagi regions.

trace the relative chronology of folding. The asymmetry of the folds, and curvature of hinge lines, suggest that the axial planes and hinge lines rotated during progressive dextral shearing.

An upward decrease of interlimb angles, and an increase in the degree of asymmetry of a given generation of folds, suggest that the present configuration of the folds has probably resulted from a single progressive deformation (D_1), rather than a series of discrete, temporarily separated tectonic events. The development of the S_1, S_2 and S_3 cleavages, stretching mineral lineations and F_1, F_2 and F_3 folds within the dynamothermal metamorphic sole can be attributed to deformation phases D_{1a}, D_{1b} and D_{1c}, respectively. There is no significant change in the metamorphic mineral assemblage between the three phases; thus, D_{1a}, D_{1b} and D_{1c} probably do not represent independent deformation phases, but rather continuous structural events. Because the greenschist facies rocks were accreted to the base of the overriding plate later than the amphibolite facies rocks, the absolute timing of the deformation phases D_{1a}, D_{1b} and D_{1c} in the former may not coincide with that in amphibolite facies counterparts.

Microscopic kinematic indicators

Shear sense directions in the dynamothermal metamorphic sole were determined from the kinematic indicators observed in oriented thin sections. Thin sections were cut parallel to the mineral stretching lineation and perpendicular to the principal foliation. In geographical terms, all projections and thin section photomicrographs

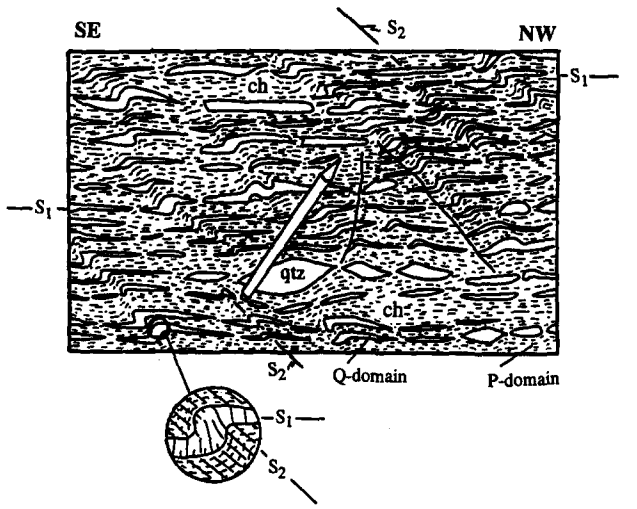

Fig. 6. Field sketch of the differentiated/metamorphic compositional layering and boudin structures in upper greenschist facies metapelites. The dark layers represent *P*-domains (ch), whereas the light layers represent *Q*-domains (qtz). The S_2 cleavage is axial planar to F_1 folds. Cleavage refraction between two domains is shown in the enlarged sketch. Pen is about 15 cm.

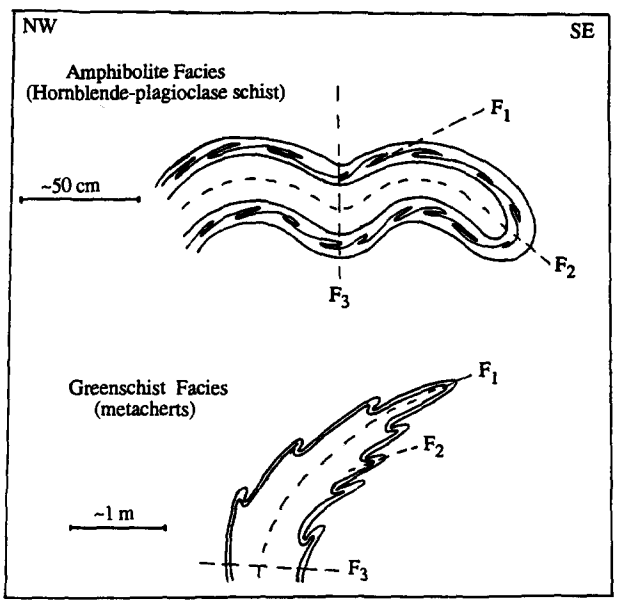

Fig. 7. Schematic representation of F_1, F_2 and F_3 folds within the amphibolite and greenschist facies rocks of the metamorphic sole.

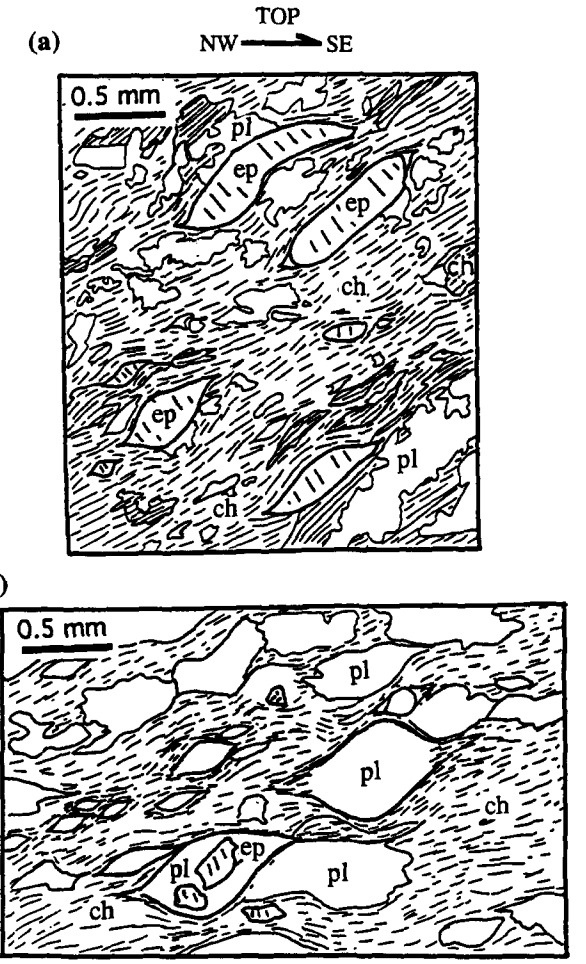

Fig. 8. Line drawing from microscopic observations of porphyroblastic epidote (a) and plagioclase (b) grains within the greenschist facies metavolcanics. Both diagrams indicate a dextral sense of shearing from northwest to southeast (ep = epidote, ch = chlorite, qtz = quartz, pl = plagioclase).

are viewed towards the northeast. In general, kinematic indicators are less clear and abundant in amphibolite facies rocks than greenschist facies rocks. Several kinematic indicators were recognized, and used to determine the prevailing shear sense during the development of the dynamothermal metamorphic sole, as follows:

Sense of fold overturning. In addition to mesoscopic scale asymmetric folds, greenschist facies rocks, particularly the metavolcanics and metapelites, are characterized by well-developed microscopic scale overturned asymmetric folds, wherever metamorphic compositional layering is readily seen. The degree of asymmetry of the microscopic folds increases from the base to the top in the greenschist facies as in the case of mesoscopic folds. Study of a large number of these folds indicates a dextral shear sense, top to the south-southeast (Fig. 11a).

Asymmetrical porphyroblast/porphyroclast structures. In the dynamothermal metamorphic sole, asymmetric porphyroblast/porphyroclast structures are dominantly of the σ-type (see Passchier & Simpson 1986), and mostly occur in greenschist facies metavolcanics and amphibolite facies gneisses. These σ-type porphyroblast/porphyroclast structures are characterized by epidote and plagioclase grains with chlorite tails in the greenschist facies metavolcanic rocks, and feldspar grains with muscovite tails in the amphibolite facies gneisses (Fig. 8). Their monoclinic asymmetry suggests that these porphyroblast/porphyroclast pressure shadow structures were formed by non-coaxial, dextral shearing (Fig. 8; see Passchier & Simpson 1986, Passchier *et al.* 1990).

Book-shelf structures. In lower greenschist facies metavolcanic rocks, relict igneous textures are preserved. Upward in the section, epidote becomes the dominant mineral. It is found both as vein infill and a

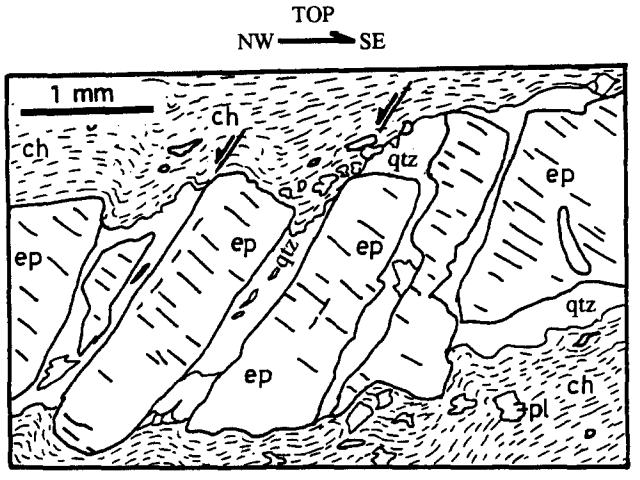

Fig. 9. Line drawing from microscopic observation of bookshelf structures in greenschist metavolcanics. Epidote veins underwent brittle deformation during which the veins were fractured, and the fragments of the veins were displaced along antithetic shear planes. The fractures are filled with quartz (ep = epidote, qtz = quartz, pl = plagioclase, ch = chlorite).

porphyroblast mineral within a chloritic matrix. Geometric relationships between the epidote veins and principal foliation, S_1, suggest that the veins are oriented at low angles to the shear plane (flow plane). In many cases, the epidote veins are broken and displaced along high angle antithetic shear planes, representing a bookshelf structure (Fig. 9; see Simpson & Schmid 1983, Passchier *et al.* 1990, Hanmer & Passchier 1991). The clockwise rotation of the epidote vein fragments indicates an overall dextral shear sense, from the top to the south-southeast, which is consistent with the shear sense deduced from epidote porphyroblast pressure shadow structures in the same samples.

Extensional shear bands. Within greenschist metavolcanic rocks, extensional shear bands tend to occur within narrow shear zones, up to several cm wide. In these shear zones, it appears that S_2 corresponds to extensional crenulation cleavage (Fig. 10; see Platt and Vissers 1980, White *et al.* 1980). The geometrical relationships between shear plane and S_1 and S_2 planar surfaces reveal a dextral displacement from north-northwest to south-southeast (see Hanmer & Passchier 1991).

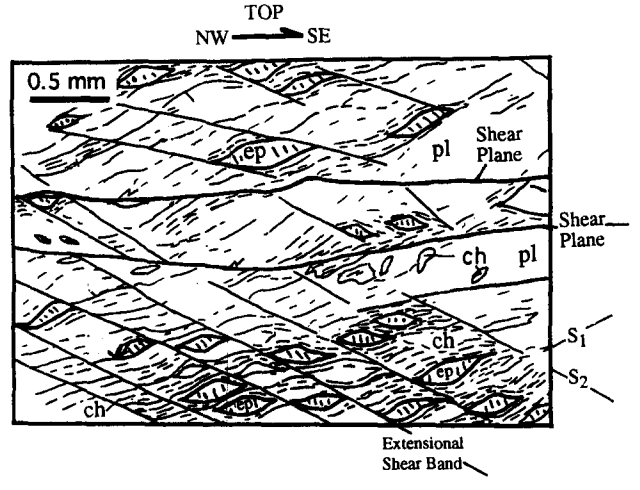

Fig. 10. Line drawing from microscopic observation of extensional shear bands, corresponding to S_2.

Mica fish structures. Mica fish structures are commonly seen within the amphibolite facies gneisses (see Lister & Snoke 1984, Hanmer & Passchier 1991, Barker 1990, Yamamoto 1994). They appear to have developed where pre-existing large muscovite grains were deformed through a combination of brittle and ductile processes. The sense of displacement in the mica fish structures is consistent with those deduced from porphyroblast/porphyroclasts and quartz *c*-axis fabrics in these rocks, indicating a dextral shearing from north-northwest to south-southeast (Fig. 11b).

Quartz c-axis fabrics. Out of nine quartz-rich samples, only three show strongly preferred quartz *c*-axis orientation and monoclinic asymmetry (Fig. 4, Fig. 11c & d; AP31A, AP16, MS-54). Sample AP31A represents the quartz–muscovite–feldspar gneisses of the amphibolite facies rocks, and is characterized by a well-developed recrystallization texture (Fig. 11c; see Urai *et al.* 1986). Samples AP16 and MS-54, with dominant quartz ribbon structures, represent mylonitic shear zones in greenschist facies rocks (Fig. 11d). The grain size in the ribbons increases from edges to centres with increasingly strong preferred orientation (Fig. 11d). This grain size increment may have been generated by incorporation of several small grains into larger ones through dynamic recovery (see Bauchez 1977, Schmid & Casey 1986).

The *c*-axis fabric skeletons of the three samples resemble the type-I crossed girdles of Lister & Hobbs (1980). As shown in Fig. 4, there is progressively developed asymmetry of the quartz *c*-axis fabrics from the lower greenschist facies to the upper amphibolite facies, as represented by the samples AP16, MS-54, and AP31A, respectively, suggesting non-coaxial progressive deformation (see Boullier & Quenardel 1981, Evans & White 1984, Law 1987, Klaper 1988, Sakakibara *et al.* 1992, Peterson & Robinson 1993).

In conclusion, the microscopic kinematic indicators and quartz *c*-axis fabrics in the dynamothermal metamorphic sole beneath the P–K ophiolite are all consistent with a NNW–SSE tectonic transport direction of the ophiolite during its intra-oceanic transport.

MÉLANGE

The Aladag mélange has been divided into three tectono-stratigraphic units based upon: (1) the lithological character and origin of the blocks and surrounding matrix; (2) deformation style (i.e. ductile vs brittle); and (3) field relationships. This sub-division reveals a tectono-stratigraphic superposition of apparently chaotic masses and also provides an insight into accretionary processes during the ophiolite emplacement (cf. Hsu 1968). Such sub-division, based upon this field study, is also consistent with the geochemical signature of the

different tectonic units (Polat 1992). The matrix of the mélange ranges from serpentinitic at the top to pelitic at the base. The blocks are predominantly exotic with respect to the surrounding matrix, and range from several tens of cm to several hundreds of m in size. Structural data representing both the linear and planar fabrics occurring in the three tectonic slices of the mélange are displayed, according to their relative position, in a measured tectonostratigraphic section (Fig. 13).

Upper tectonic slice

The matrix of the upper tectonic slice of the mélange is characterized by ductilely deformed serpentinitic mylonite. The blocks are composed mainly of pillow lava, gabbro, peridotite and metamorphosed rocks, volcanic and sedimentary in origin. They are generally lenticular in shape and variable in size, ranging from a few m to several tens of m, and are separated by the curviplanar ductile shear zones. The intensity of deformation in this tectonic slice increases towards the overlying dynamothermal metamorphic sole and ophiolite.

Well-developed penetrative cleavage, ranging from rhombohedral to phacoidal (scaly), is the most striking structural characteristic of the upper tectonic slice (Figs. 12a & b). With increasing intensity of deformation, the rhombohedral cleavage grades into phacoidal cleavage. The rhombohedral cleavage primarily occurs outside of the shear zones, whereas the phacoidal cleavage is closely associated with the shear zones. Within the shear zones, the penetrative phacoidal cleavage wraps around inequant, isolated, ellipsoidal or augen-shaped clasts of gabbro and peridotite. Many foliation surfaces are polished and exhibit well-developed striations. Ductile shear zones occasionally exhibit *S–C* composite planar fabrics. Most of the augen-shaped clasts tend to have asymmetric tails, and are associated with *S–C* planar surfaces. Small veins of magnesite, whose thickness ranges from several mm to several cm, are abundant in peridotitic blocks, and generally tend to make angles of 70–90° with the surrounding shear planes.

Several types of consistently oriented planar and linear structures were used to determine the tectonic transport direction in this tectonic slice. The planar structures include: *S–C* fabrics and NE-striking, SE–NW-dipping curviplanar ductile shear zones (Figs. 12c and 13a; see Berthé *et al.* 1979). The linear structures are: NW–SE-trending slickenside lineations (Fig. 13b), long axis preferred shape orientation of the NW–SE-trending and mostly SE-plunging pebble to cobble size fragments (Figs. 12d and 13c), elongated amygdules and vesicules in the pillow lava blocks, and asymmetric augen structures (Fig. 12e). These structures are well exposed in the vicinity of Camlica and indicate that the overriding plate moved from northwest to southeast (Figs. 5 and 13).

Collectively, the presence of highly polished and striated slickensides, strongly oriented clasts, *S–C* composite planar fabrics and augen structures within a strongly foliated serpentinitic matrix are consistent with a tectonic origin for the upper tectonic slice of the Aladag mélange. The characteristics of the block and matrix lithologies suggest that this tectonic slice of the mélange may have formed in an oceanic environment prior to the obduction of the ophiolite onto the continental margin.

Middle tectonic slice

In contrast to the upper tectonic slice, this slice is characterized by a less-foliated matrix of turbidites, with some recognizable Bouma sequences. The blocks are composed of tectonic breccia, serpentinite, amphibolite and greenschist facies metamorphic rocks, and carbonates, suggesting an exotic origin of the blocks with respect to the surrounding matrix.

The major structures in the middle tectonic slice are characterized by a series of NE-trending, SE-verging close to tight asymmetric folds and associated NW-dipping, NE-striking thrust faults, suggesting a SE-directed tectonic transport (Fig. 12f). The fold axes are generally horizontal, with an average plunge of 2° towards N38°E (Fig. 13e). Similarly, stylolites, developed as pressure solution cleavage in the limbs of the folds, indicate that the main compressional direction was NNW–SSE during folding. Thrust faults occur mainly along the long limbs of asymmetric folds. Poles to the axial planes and thrust surfaces are shown in Figs. 13(d) & (f).

Lower tectonic slice

The lower tectonic slice of the mélange complex is a chaotic unit with dominantly brittle deformation. The matrix is characterized by turbiditic shales and sandstones at the top, and locally exposed cataclasite at the base. The blocks are composed of limestones, cherts, and volcanic rocks, mainly oriented in a SW–NE direction. Petrographic analysis of the cataclastic matrix reveals that it resulted from brittle disaggregation of limestone, dolomite, chert and volcanic blocks.

Most of the blocks are lensoidal in shape and are separated predominantly by NE-striking, moderately to steeply SE-dipping, brittle shear zones (Fig. 13g). The strongly polished surfaces of the chert blocks exhibit well-developed NW–SE-trending slickenside lineations (Fig. 13h). The number of carbonate blocks increases towards the base and some of them are laterally transitional into the underlying para-autochthonous nappes. The shear zones separating the blocks are parallel to the lower tectonic boundary. The en-échelon tension gashes within the blocks and immediately underlying carbonates reveal that shearing was top to the south-southeast.

CONCLUSIONS

The Aladag region of eastern Taurides, Turkey, represents one of the best areas in which to study the

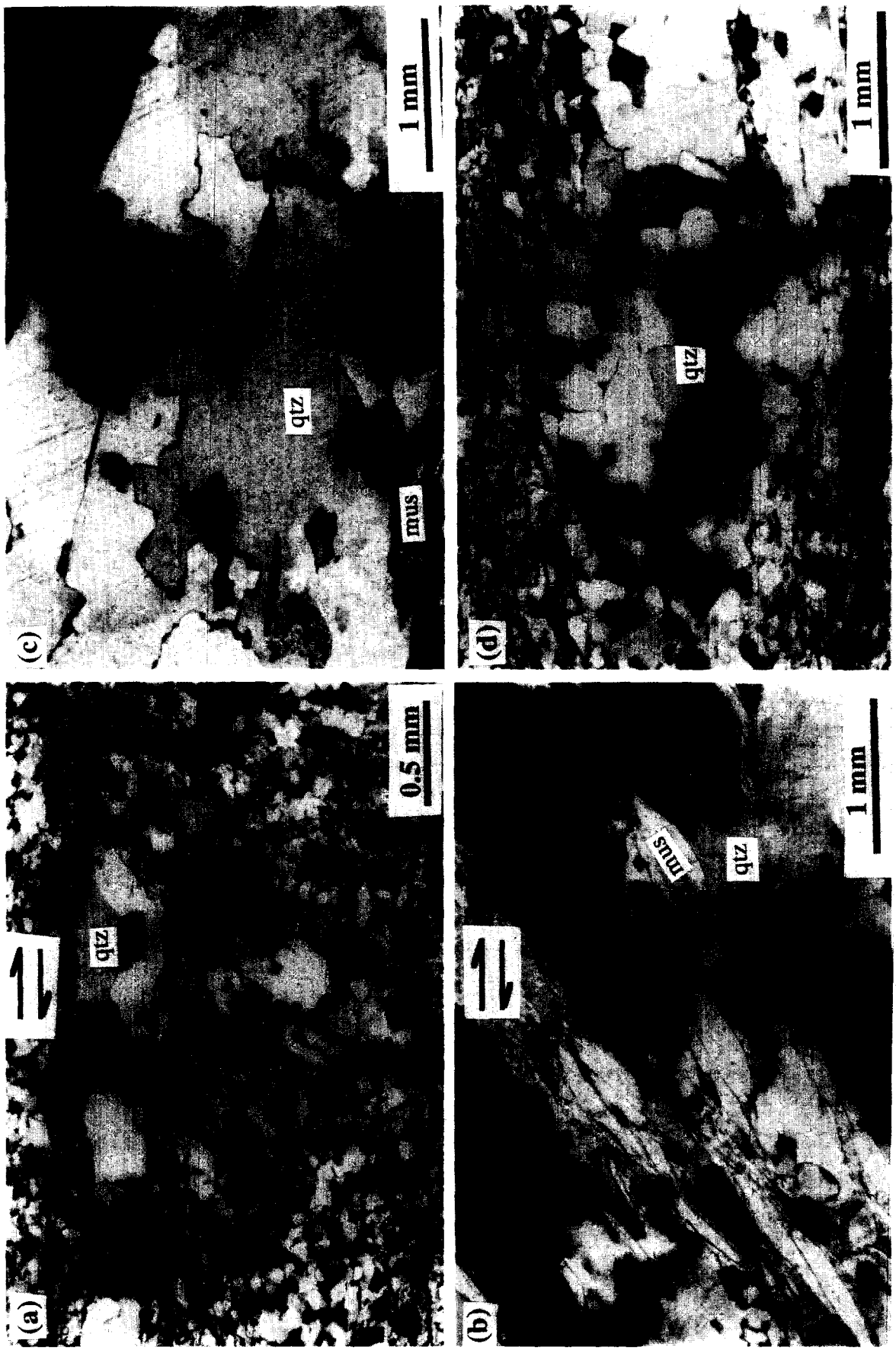

Fig. 11. Photomicrographs of the dynamothermal metamorphic sole. (a) An asymmetric overturned fold in greenschist facies metapelites. (b) Mica fish structures developed in the quartz–muscovite–feldspar gneiss of the amphibolite grade. (c) Dynamic recrystallization characterized by grain boundary migration (shady field along the grain boundaries) and deformation lamellae in the quartz–muscovite–feldspar gneiss. (d) Quartz ribbons in mylonites developed along shear zones in the greenschist facies rocks, the grain size increases towards the centre of the ribbon. In geographical terms all photomicrographs are viewed towards the northeast. Photomicrographs (a) and (b) exhibit a right-lateral shear sense, indicating that the top layer moved from the northwest to the southeast (qtz = quartz, mus = muscovite).

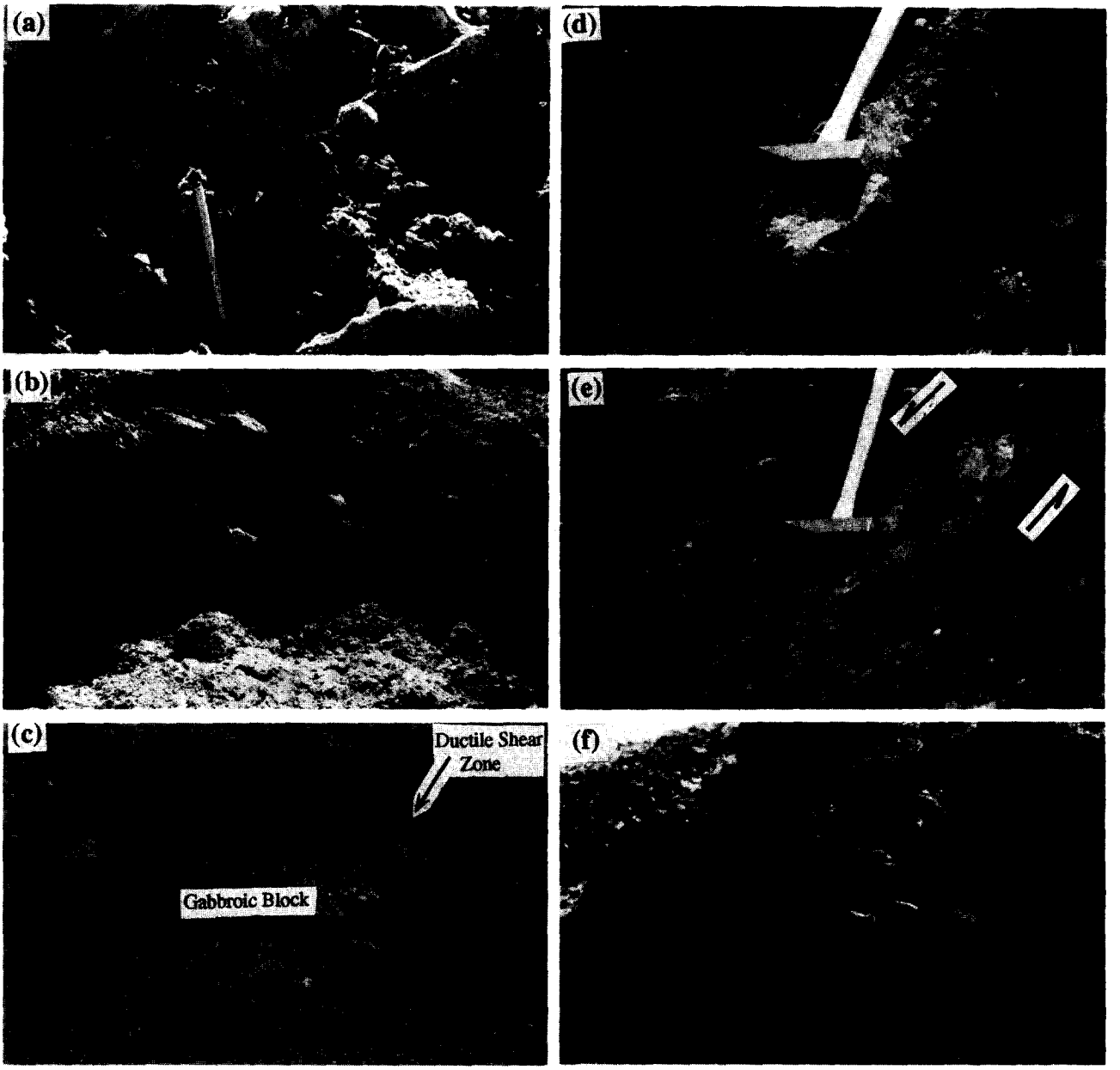

Fig. 12. Field photographs of the mélange. (a) Rhombohedral cleavage. (b) Phacoidal (scaly) cleavage. (c) A ductile shear zone surrounding a gabbroic block. (d) Preferred long axis orientation of a peridotite fragment within the serpentinitic matrix. (e) An augen structure, viewed towards the southwest. (f) Folding and fracturing in the micritic limestone also viewed towards the southwest.

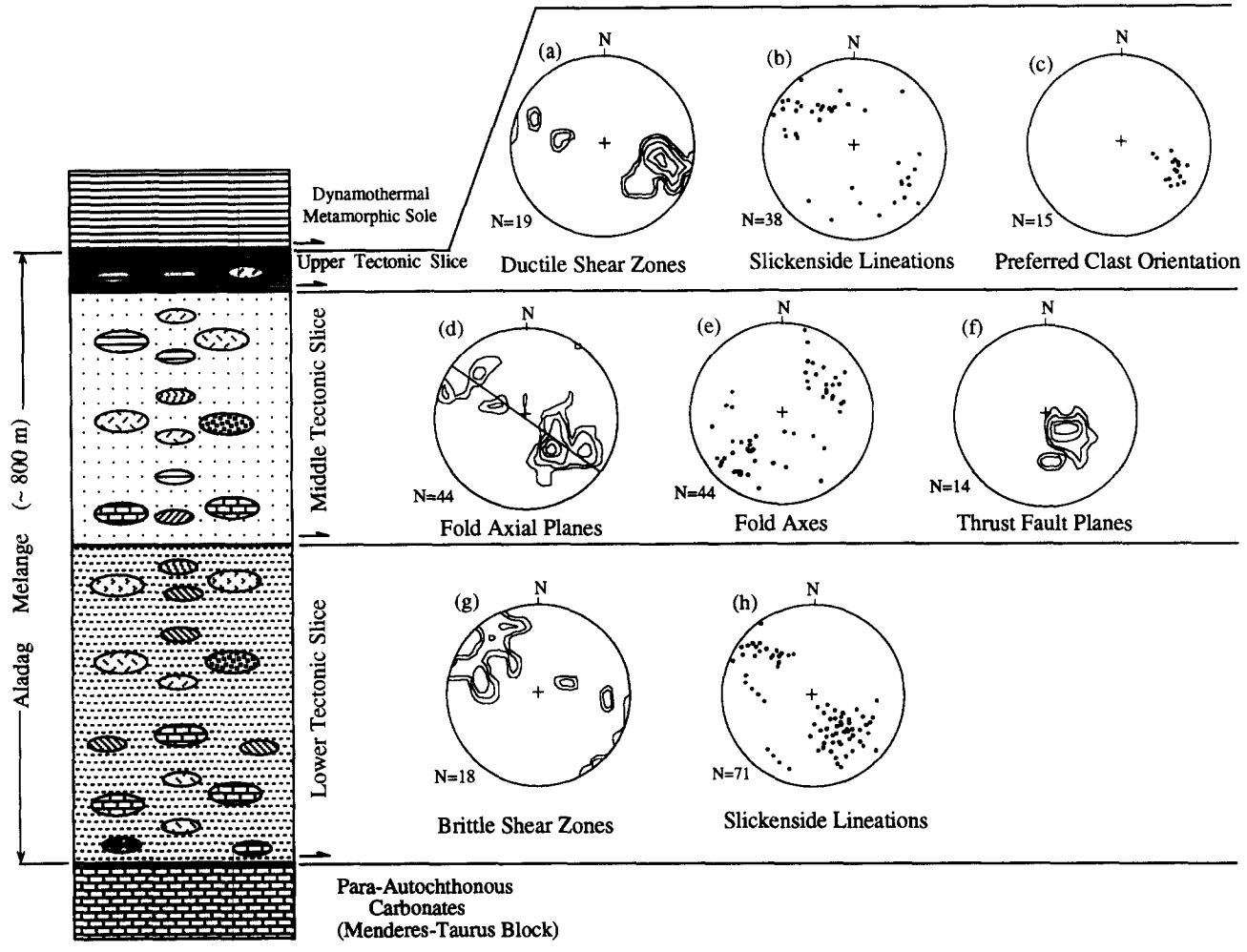

Fig. 13. Tectonostratigraphic section of the Aladag mélange and equal-area, lower hemisphere plots of the linear and planar structures within the upper, middle, and lower tectonic slices. (a) Poles to the ductile shear zones. (b) Slickenside lineations developed on the shear planes of serpentinitic matrix. (c) Preferred long-axis orientation of the pebble to cobble size fragments. (d) Poles to the fold axial planes (contour interval is 2% per 1% area). (e) Fold axes. (f) Poles to the thrust faults associated with SE-verging folds. (g) Poles to the brittle shear zones. (h) Slickenside lineations developed along the brittle shear planes. Contour interval is 2% per 1% area.

geological history of the emplacement of a Tethyan-type ophiolite onto a passive continental margin by a pre-terminal collisional event. Analyses of the attitudes of the structural fabrics and kinematic indicators, both within the dynamothermal metamorphic sole and the underlying mélange beneath the P–K ophiolite, are collectively consistent with SSE-directed tectonic transport prevailing during the emplacement of the ophiolite onto the M–T block in the Late Cretaceous (Fig. 14).

The emplacement history of the P–K ophiolite onto the M–T continental block is recorded by metamorphism and associated deformation within the ophiolite itself, and in the high to low temperature accreted thrust units beneath the ophiolite. In the dynamothermal metamorphic sole and Aladag mélange, the degree of metamorphism and intensity of deformation progressively decrease from top to base, suggesting that the emplacement of the ophiolite was a relatively continuous geodynamic event. This may have included: (1) decoupling of relatively young oceanic lithosphere, which is recorded by the several m of mantle tectonite between the ophiolite and the dynamothermal metamorphic sole; (2) a period of intra-oceanic subduction and transport of the overriding oceanic plate towards the M–T continental margin, which is represented by the dynamothermal metamorphic sole and upper tectonic slice of the mélange; and finally (3) 'obduction' onto the M–T continental block by a pre-terminal collision, which is characterized by the formation of the lower tectonic slice of the mélange and SSE-verging imbricated thrust structure of the region. Decrease of metamorphic grade and intensity of deformation from top to base in the dynamothermal metamorphic sole may have resulted from cooling and structural thinning of the overriding plate during its intra-oceanic transport (cf. Casey & Dewey 1984). Variation of deformation style from ductile at the top to brittle at the base in the Aladag mélange likely stemmed from uplift of the overriding oceanic lithosphere on top of relatively less dense and more buoyant passive continental margin of the M–T block when the latter attempted to subduct beneath the denser P–K ophiolitic complex during the preterminal collision. Development of the imbricated thrust structures can be attributed to gravity sliding of the uplifted P–K ophiolite towards the centre of the M–T block (cf. Dewey 1976).

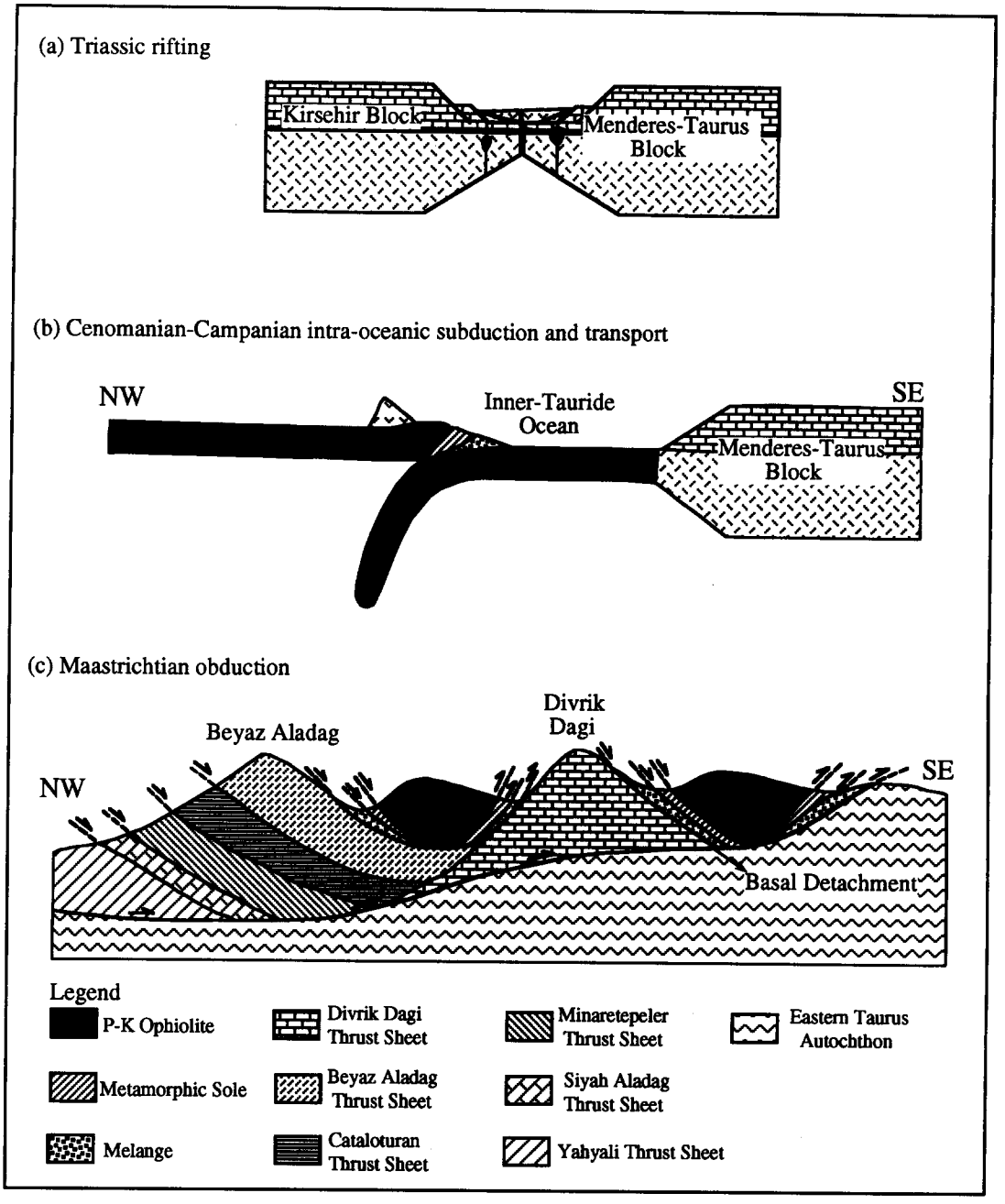

Fig. 14. (a) Schematic representation of the Triassic rifting and separation of the Menderes–Taurus block from the Kirsehir block. (b) Schematic illustration of the formation of the dynamothermal metamorphic sole and mélange beneath the Pozanti–Karsanti ophiolite during its intra-oceanic transport stage. (c) Simplified NW–SE cross-section of the study area, showing the thrust structures developed during the last stage emplacement of the Pozanti–Karsanti ophiolite from the northwest onto the Menderes–Taurus continental block in the late Cretaceous (Maastrichtian?).

The litho-tectonostratigraphy and geometry of the structures in the Aladag region are strikingly similar to those developed in other ophiolite obduction-related orogenic belts, such as the Semail Ophiolite of Oman, the Bay of Island ophiolite of western Newfoundland, and Papua ophiolite of New Guinea (Dewey 1976, Robertson *et al.* 1990, Searle *et al.* 1990, Jones & Robertson 1991, Sengör 1990a). Results of this study suggest that structural analyses in dynamothermal metamorphic soles and underlying mélanges beneath Tethyan-type ophiolites can contribute to an understanding of the tectonic history of obduction-related orogenic belts.

Acknowledgements—The authors thank A. M. C. Sengör, M. R. Stauffer and R. Kerrich for incisive critique of an initial draft, and suggestions which have greatly improved the initial draft manuscript. Incisive and comprehensive critiques by journal reviewers, M. C. Blake Jr, R. J. Norris and P. A. Cawood have resulted in significant improvement of the paper. This research was funded by the National Science Foundation Grant EAR 8721166.

REFERENCES

Barker, A. J. 1990. *Introduction to Metamorphic Textures and Micro Structures*. Blackie & Son Ltd, New York.

Berthé, D., Choukroune, P. & Jegouze, P. 1979. Orthogneiss, mylonite and non-coaxial deformation of granites: the example of the south Armorican shear zone. *J. Struct. Geol.* **1**, 31–42.

Blumenthal, M. M. 1947. Belemedik Paleozoik penceresi ve bunun Mesozoik kalker çevresi (Klikya Toroslari). *M.T.A. yayinlari, Seri D* **3**.

Boote, D. R., Mou, D. & Waite, R. I. 1990. Structural evolution of the Suneinah Foreland, Central Oman mountains. In: *The Geology and Tectonics of the Oman Region* (edited by Robertson, A. H. F., Searle, M. P. & Ries, A. C.). *Spec. Publ. geol. Soc. Lond.* **49**, 397–418.

Bouchez, J. L. 1977. Plastic deformation of quartzites at low temperature in an area of natural strain gradient (Angres, France). *Tectonophysics* **39** 25–50.

Boullier, A. M. & Quenardel, J. M. 1981. The Caledonides of northern Norway: relation between preferred orientation of quartz lattice and translation of nappes. In: *Thrust and Nappe Tectonics* (edited by McClay, K. P. & Price, N. J.). *Geol. Soc. Lond. Spec. Publ.* **9**, 185–195.

Byrne, T. 1984. Early deformation of mélange terranes of Ghost Rock Formation, Kodiak Island, Alaska. In: *Mélanges* (edited by Raymond, L. A.). *Spec. Pap. geol. Soc. Am.* **198**, 21–51.

Casey, J. F. & Dewey, J. F. 1984. Initiation of subduction zones along transform and accreting plate boundaries, triple-junction evolution and forearc spreading centers—implication for ophiolitic geology and obduction. In: *Ophiolites and Oceanic Lithosphere* (edited by Gass, I., G. Lippard, S. J. & Shelton, A. W.). *Spec. Publ. geol. Soc. Lond.* **13**, 269–290.

Coleman, R. G. 1971. Plate tectonic emplacement of upper mantle peridotites along continental edges. *J. geophys. Res.* **76**, 1212–1222.

Coleman, R. G. 1977. *Ophiolites*. Springer-Verlag, New York.

Coleman, R. G. 1981. Tectonic setting for ophiolite obduction in Oman. *J. geophys. Res.* **86**, 2497–2508.

Delaloye, M. & Wager, J. J. 1984. Ophiolite and volcanic activity near the western edge of the Arabian plate. In: *The Geological Evolution of the Eastern Mediterranean* (edited by Dixon, J. F. & Robertson, A. H. F.). *Spec. Publ. geol. Soc. Lond.* **17**, 225–249.

Dercourt, J. 1986. Geologic evolution of the Tethys from the Atlantic to the Pamirs since Lias. *Tectonophysics* **123**, 241–315.

Dewey, J. F. 1976. Ophiolite obduction. *Tectonophysics* **31**, 93–120.

Dewey, J. F. 1988. Lithospheric stress, deformation and tectonic cycles: the disruption of Pangea and the closure of Neo-Tethys. In: *Gondwana and Tethys* (edited by Audley-Charles, M. G. & Hallam, A.). *Spec. Publ. geol. Soc. Lond.* **37**, 23–40.

Dewey, J. F. & Bird, J. M. 1971. Origin and emplacement of the ophiolite suite: Appalachian ophiolites in Newfoundland. *J. geophys. Res.* **76**, 3179–3206.

Evans, D. J. and White, S. H. 1984. Microstructural and fabric studies from the rocks of the Moine Nappe, Erribol, NW Scotland. *J. Struct. Geol.* **8**, 369–389.

Görür, N., Oktay, F. Y., Seymen, I. & Sengör, A. M. C. 1984. Paleotectonic evolution of the Tuzgölü basin complex, Central Turkey: sedimentary record of a Neo-Tethyan closure. In: *The Geological Evolution of the Eastern Mediterranean* (edited by Dixon, J. F. & Robertson, A. H. F.). *Spec. Publ. geol. Soc. Lond.* **17**, 467–482.

Hacker, B. R. 1990. Simulation of the metamorphic sole and deformational history of the metamorphic sole of the Oman ophiolite. *J. geophys. Res.* **95**, 4895–4907.

Hanmer, S. & Passchier, C. 1991. Shear sense indicators: a review. *Spec. Pap. Geol. Soc. Canada* **90-17**, 1–72.

Hippert, J. F. M. 1993. 'V' pull-apart microstructures: a new shear sense indicator. *J. Struct. Geol.* **15**, 1393–1403.

Hsu, K. J. 1968. Principles of mélanges and their bearing on Franciscan–Knoxville paradox. *Bull. geol. Soc. Am.* **79**, 1063–1074.

Jamieson, R. A. 1986. P–T paths from high temperature shear zones beneath ophiolites. *J. metamorph. Geol.* **4**, 3–22.

Jones, G. & Robertson, A. H. F. 1991. Tectonostratigraphy and evolution of the Mesozoic Pindos ophiolite and related units, northwestern Greece. *J. Geol. Soc. Lond.* **148**, 267–288.

Keep, M. & Hansen, V. L. 1994. Deformational style in the Proterozoic Pinal Schist, Pinal Peak, Arizona: microstructural and quartz *c*-axis analysis. *J. Geol.* **102**, 229–242.

Klaper, E. M. 1988. Quartz *c*-axis fabric development and large scale nappe folding (Wandfluhhorn fold, Penninic nappes). *J. Struct. Geol.* **10**, 795–802.

Law, R. D. 1987. Heterogeneous deformation and quartz crystallographic fabric transition: Natural examples from the Moine thrust zone at Stack of Glencoul, northern Assynt. *J. Struct. Geol.* **9**, 819–833.

Lister, G. S. & Hobbs, B. E. 1980. The simulation of fabric development and its application to quartzite: the influence of deformation history. *J. Struct. Geol.* **2**, 355–370.

Lister, G. S. & Snoke, A. W. 1984. *S–C* mylonites. *J. Struct. Geol.* **6**, 617–638.

Moores, E. M. 1982. Origin and emplacement of ophiolites. *Rev. Geophys.* **20**, 735–750.

Passchier, C. W. & Simpson, C. 1986. Porphyroclast systems as kinematic indicators. *J. Struct. Geol.* **8**, 831–843.

Passchier, C. W., Myers, J. S. & Kröner, A. 1990. *Field Geology of High Grade Gneiss Terrains*. Springer-Verlag, New York.

Peterson, V. L. & Robinson, P. 1993. Progressive evolution from uplift to orogen-parallel transport in a late-Acadian amphibolite to granulite facies shear zone, south central Massachusetts. *Tectonics* **12**, 550–567.

Platt, J. P. & Vissers, R. L. 1980. Extensional structures in anisotropic rocks. *J. Struct. Geol.* **2**, 379–410.

Polat, A. 1992. Structural and geochemical evolution of the Aladag mélange complex and greenschist division of the dynamothermal metamorphic sole beneath the Pozanti–Karsanti ophiolite, eastern Taurides, Turkey. Unpublished M.Sc. thesis, University of Houston Department of Geosciences, Houston.

Rajlich, P. 1991. Kinematics of crenulation cleavage development: examples from the Upper Devonian rocks from northeast of Bohemia Massif, Czechoslovakia. *Tectonophysics* **190**, 193–208.

Robertson, A. H. F. & Dixon, J. E. 1984. Introduction: geological evolution of the eastern Mediterranean. In: *The Geological Evolution of the Eastern Mediterranean* (edited by Dixon, J. F. and Robertson, A. H. F.). *Spec. Publ. geol. Soc. Lond.* **17**, 1–74.

Robertson, A. H. F., Blome, C. D., Cooper, D. W. J., Kemp, A. E. S. & Searle, P. 1990. Evolution of the Arabian continental margin in the Dibba zone, Northern Oman mountains. In: *The Geology and Tectonics of the Oman Region* (edited by Robertson, A. H. F., Searle, M. P. & Ries, A. C.). *Spec. Publ. geol. Soc. Lond.* **49**, 251–284.

Sakakibara, N., Hara, I., Kanai, K., Kaikiri, K., Shiota, T., Hide, K. & Paullitsch, P. 1992. Quartz microstructures of the Sambagawa schist and their implications in convergent margin processes. *The Island Arc* **1**, 186–197.

Schmid, S. M. & Casey, M. 1986. Complete fabric analysis of some commonly observed quartz *c*-axis patterns. *Am. geophys. Union Monogr.* **36**, 263–286.

Searle, M. P. & Malpas, J. 1982. Petrochemistry and origin of sub-ophiolitic metamorphic and related rocks in the Oman mountains. *J. geol. Soc. Lond.* **139**, 235–248.

Searle, M. P., Cooper, D. W. J. & Watts, K. F. 1990. Structure of the Jebel Sumeini–Jebel Ghawil area, Northern Oman. In: *The Geology and Tectonics of the Oman Region* (edited by Robertson, A. H. F., Searle, M. P. & Ries, A. C.). *Spec. Publ. geol. Soc. Lond.* **49**, 361–374.

Sengör, A. M. C. 1990a. Plate tectonics and orogenic research after 25 years: a Tethyan perspective. *Earth Sci. Rev.* **27**, 1–201.

Sengör, A. M. C. 1990b. A new model for the Late Paleozoic–Mesozoic tectonic evolution of Iran and implication for Oman. In: *The Geology and Tectonics of the Oman Region* (edited by Robertson, A. H. F., Searle, M. P. & Ries, A. C.). *Spec. Publ. geol. Soc. Lond.* **49**, 797–831.

Sengör, A. M. C. & Yilmaz, Y. 1981. Tethyan evolution of Turkey: a plate tectonic approach. *Tectonophysics* **75**, 141–181.

Shackleton, R. M., Ries, A. C., Bird, R. P., Filbrandt, J. B., Lee, C. W. & Cunningham, J. C. 1990. The Batain Mélange of NE Oman. In: *The Geology and Tectonics of the Oman Region* (edited by Robertson, A. H. F., Searle, M. P. & Ries, A. C.). *Spec. Publ. geol. Soc. Lond.* **49**, 673–696.

Simpson, C. & Schmid, S. F. 1983. An evaluation of criteria to deduce the sense of movement in sheared rocks. *Bull. geol. Soc. Am.* **94**, 1281–1288.

Spray, J. G. 1984. Possible causes and consequences of upper mantle decoupling and ophiolite displacement. In: *Ophiolites and Oceanic Lithosphere* (edited by Gass, I. G., Lippard, S. J. & Shelton, A. W.). *Spec. Publ. geol. Soc. Lond.* **13**, 255–268.

Tekeli, O. 1981. Toroslarda Aladag ofiyolitli melanjinin ozellikleri. *Turkiye Jeoloji Kurumu Bultl.* **24**, 57–64.

Tekeli, O., Aksay, A., Urgun, B. M. & Isik, A. 1983. Geology of Aladag mountains. In: *Geology of Taurus Belt Proceedings* (edited by Tekeli, O. & Göncüoglu, M. C.), pp. 143–158.

Thuizat, R., Whitechurch, H., Montigny, R. and Juteau, T. 1981. K–Ar dating of the some infra-ophiolitic metamorphic soles from the eastern Mediterranean: New evidence for intra-oceanic thrusting before obduction. *Earth Planet. Sci. Lett.* **52**, 302–310.

Urai, J. L., Means, W. D. & Lister, G. S. 1986. Dynamic recrystallization of minerals. *Am. Geophys. Union Monogr.* **36**, 161–197.

White, S. H., Burrows, S. E., Carreras, J., Shaw, N. D. & Humphreys, F. J. 1980. On mylonites in ductile shear zones. *J. Struct. Geol.* **2**, 175–187.

Whitechurch, H., Juteau, T. & Montigny, R. 1984. Eastern Mediterranean ophiolites (Turkey, Syria and Cyprus) in the history of the Neo-Tethys. In: *The Geological Evolution of the Eastern Mediterranean* (edited by Dixon, J. F. & Robertson, A. H. F.). *Spec. Publ. geol. Soc. Lond.* **17**, 301–317.

Williams, P. F. 1990. Differentiated layering in metamorphic rocks. *Earth Sci. Rev.* **29**, 267–281.

Williams, H. & Smyth, W. R. 1973. Metamorphic aureoles beneath ophiolite suites and alpine peridotites: tectonic implications with west Newfoundland examples. *Am. J. Sci.* **273**, 594–621.

Yamamoto, H. 1994. Kinematics of mylonitic rocks along the median tectonic line, Akaishi Range, central Japan. *J. Struct. Geol.* **16**, 61–70.